Lattice-dynamical model for the elastic constants and Raman frequencies in $(V_{1-x}Cr_x)_2O_3$

H. Yang and R. J. Sladek
Department of Physics, Purdue University, West Lafayette, Indiana 47907
(Received 14 May 1985)

We report the first lattice-dynamical study of V_2O_3 and $(V_{0.985}Cr_{0.015})_2O_3$ in the long-wavelength limit using a rigid-ion model with an effective ionic charge and various short-range interactions. The parameters of the model were determined from nonlinear least-squares fits to the experimental elastic constants and the frequencies of Raman-active modes at room temperature. The validity of the model was established by verifying that the calculated elastic constants and Raman frequencies were in good agreement with experimental data for V_2O_3 and $(V_{0.985}Cr_{0.015})_2O_3$ as well as for Al_2O_3 to which the same model was also applied. The effective ionic charge of each $(V_{1-x}Cr_x)_2O_3$ crystal was found to be considerably larger than that of Al_2O_3 in accordance with the ionicity of V_2O_3, estimated from the dielectric theory of Levine, being larger than that of Al_2O_3. The short-range force constants of $(V_{1-x}Cr_x)_2O_3$ were found to be quite different from those of Al_2O_3. It was also found that most of the model parameters for semiconducting $(V_{0.985}Cr_{0.015})_2O_3$ have values in between those of metallic V_2O_3 and insulating Al_2O_3. The effect of alloying a small amount of Cr_2O_3 into V_2O_3 on the interatomic force-field parameters is also discussed.

I. INTRODUCTION

Corundum-structured $(V_{1-x}Cr_x)_2O_3$ has been studied extensively[1,2] since the discovery of the metal-insulator transition in 1969. It was found that this transition can be induced by a change in temperature, pressure, or composition.[3] Despite this strong interest in many properties of this compound, lattice-dynamical studies have been very scarce due primarily to a lack of complete information about the vibrational spectra as well as to a rather complicated crystal structure and the presence of d electrons. Infrared-absorption[4] and reflectivity[5] measurements on $(V_{1-x}Cr_x)_2O_3$ crystals yielded only a few phonon peaks with not so well defined frequencies, probably due to the relatively high conductivity of these crystals obscuring the vibrational effects, while neutron-scattering experiments[6,7] for these crystals were limited to some of the acoustic branches. However, Raman spectra of $(V_{1-x}Cr_x)_2O_3$ have been studied[8,9] in detail to identify the frequencies of zone-center optical phonons belonging to the A_{1g} and E_g species. Furthermore, the measurements of all six independent elastic constants have also been carried out not only for pure V_2O_3,[10,11] but also for Cr-doped V_2O_3.[12]

The purpose of the work presented in this paper was to construct a lattice-dynamical model in the long-wavelength limit which could reproduce both the experimental elastic constants and the frequencies of Raman-active modes for the $(V_{1-x}Cr_x)_2O_3$ crystals. The model is basically similar to that used by Striefler and Barsch[13] for rutile-structured fluorides extended to the corundum structure. Explicit expressions for the external- and internal-strain contributions to the elastic constants and for the frequencies of Raman-active vibrations will be derived using the "long-wave method" of Born and Huang[14] based on the rigid-ion approximation. The expressions contain the effective charge parameter for Coulomb interaction and the short-range parameters for two-body central forces and three-body bond-bending forces between neighboring atoms. The absence of information on the frequencies of infrared-active vibrations does not present a serious problem in this model because in the corundum structure, which has a center of inversion symmetry, Raman-active modes and infrared-active modes are mutually exclusive and, consequently, the internal-strain contributions to the elastic constants depend solely on the frequencies of Raman-active modes.[15] It is noted that at present there seems to be no simple method to incorporate the presence of d electrons into the model. Although the alloying of small amount of Cr_2O_3 into V_2O_3 is known[2] to alter the electronic band structure resulting in a drastic increase in the electrical resistivity (from a metallic to an insulating phase), it is not expected to affect the lattice properties significantly.

To test the general validity of the present model, it was also applied to an isostructural compound Al_2O_3, for which other investigators have used various rigid-ion[16,17] or polarizable-ion[17,18] models to interpret lattice-vibrational spectra.

II. THEORETICAL MODEL

A. Crystal structure

The α-corundum structure M_2O_3 consists of a primitive rhombohedral lattice with two formula units per cell as shown in Fig. 1(a).[19] The positions of atoms within a unit cell are completely specified by four structural parameters, i.e., a, c, u, and v, where a and c are lattice constants (hexagonal indexing) and u and v are positional parameters for cations and anions, respectively. With the center of inversion taken as the origin and the twofold axis as the x axis, cations $M(1)$ and $M(2)$ are located at

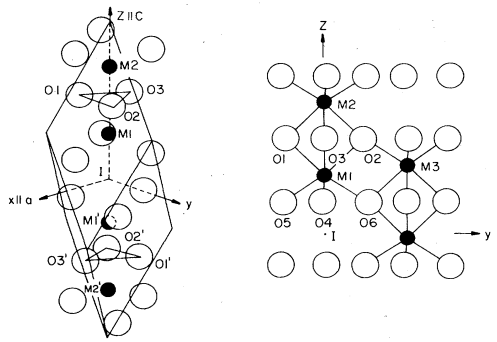

FIG. 1. (a) The rhombohedral unit cell of the α-corundum structure which contains two formula units of M_2O_3. (b) The projection of the α-corundum structure on a mirror plane perpendicular to the twofold axis. Only the atoms in the upper half of a unit cell and their typical nearest neighbors are labeled.

TABLE I. The structural parameters (structural parameters are from Refs. 21 (V_2O_3), 22 [$(V_{0.985}Cr_{0.015})_2O_3$], and 23 ($Al_2O_3$)) ($a$,$c$, $r=c/a$, u, and v), Madelung constant (M), and derivatives of M with respect to the structural parameters (M_r, M_u, and M_v) for V_2O_3, $(V_{0.985}Cr_{0.015})_2O_3$, and Al_2O_3.

	V_2O_3	$(V_{0.985}Cr_{0.015})_2O_3$	Al_2O_3
a (Å)	4.9492	4.9978	4.7589
c (Å)	13.998	13.932	12.991
r	2.823	2.7876	2.7298
u	0.0963	0.0986	0.102
v	0.3122	0.3077	0.306
M	30.7416	30.9639	31.2197
M_r	−3.5851	−3.5922	−3.5102
M_u	19.9054	13.3688	10.3510
M_v	−9.9224	−7.5313	−3.6748

$(0,0,(\frac{1}{4}-u)r)$ and $(0,0,(\frac{1}{4}+u)r)$, respectively, and anions O(1), O(2), and O(3) are at $(\frac{1}{2}v,-(\sqrt{3}/2)v,\frac{1}{4}r)$, $(\frac{1}{2}v,(\sqrt{3}/2)v,\frac{1}{4}r)$, and $(-v,0,\frac{1}{4}r)$, respectively, in units of a with $r=c/a$.[20] The coordinates of the five remaining ions (labeled with primed numbers) can be readily obtained by inversion symmetry. The projection of the corundum structure on a mirror plane perpendicular to the twofold axis is shown in Fig. 1(b),[21] where only the ions in the upper half of a unit cell and their typical nearest neighbors are labeled.

There are two different cation-anion distances,

$$R_1=R(M(1)-O(4))=(v^2-v+s-t+w)^{1/2}\,, \tag{1a}$$

$$R_2=R(M(1)-O(1))=(v^2+s)^{1/2}\,, \tag{1b}$$

two different cation-cation distances,

$$R_3=R(M(1)-M(2))=2ur\,, \tag{2a}$$

$$R_4=R(M(1)-M(3))=(4s-2t+\omega)^{1/2}\,, \tag{2b}$$

and four different anion-anion distances,

$$R_5=R(O(1)-O(2))=\sqrt{3}v\,, \tag{3a}$$

$$R_6=R(O(1)-O(4))=(4v^2-2v+w)^{1/2}\,, \tag{3b}$$

$$R_7=R(O(1)-O(5))=(v^2-v+w)^{1/2}\,, \tag{3c}$$

$$R_8=R(O(1)-O(6))=(v^2+s)^{1/2}\,, \tag{3d}$$

where all distances are in units of a with $s=u^2r^2$, $t=\frac{1}{3}ur^2$, and $w=(\frac{1}{6}r)^2+\frac{1}{3}$. The numerical values of the structural parameters are listed in Table I for V_2O_3, $(V_{0.985}Cr_{0.015})_2O_3$, and Al_2O_3. Also included in Table I are Madelung constants and their derivatives with respect to the structural parameters which will be required for the equilibrium conditions specified in the following section.

B. Parameters of the model

The potential energy per unit cell of the corundum-type sesquioxides can be written, taking into account a partly ionic and partly covalent nature of atomic bonding, as[14,24]

$$\Phi=\Phi^C+\Phi^{SR}\,. \tag{4}$$

The first term is the Coulomb energy, which, in the rigid-ion approximation, can be written as

$$\Phi^C=-\frac{M(zq)^2}{a}\,, \tag{5}$$

where M is the Madelung constant, q ($=-2|e|$) the smallest charge in the lattice, z the effective charge parameter, and a an arbitrary distance chosen as lattice constant a. The second term in Eq. (4) represents the short-range repulsive energy which is assumed to be made up of two-body central interactions and three-body, bond-bending interactions between near neighbors so that

$$\Phi^{SR}=\sum_{i=1}^{8} n_i\phi_i(R_i)+\Phi^B\,, \tag{6}$$

where $\phi_i(R_i)$ is a pair potential for atoms with interatomic distance R_i, and $n_i=12$, 12, 6, 2, 6, 6, 12, and 12, respectively, for $i=1$–8. Since the exact forms of these ϕ_i's are not known, we will assume for simplicity that they are axially symmetric and define their first and second derivatives in terms of dimensionless parameters, A_i's and B_i's, as

$$\frac{e^2}{a^3}A_i=\left[\frac{\partial^2\phi_i(R)}{\partial R^2}\right]_{R=R_i}\,, \tag{7a}$$

$$\frac{e^2}{a^3}B_i=\left[\frac{1}{R}\frac{\partial\phi_i(R)}{\partial R}\right]_{R=R_i}\,, \tag{7b}$$

where $i=1$–5 and the short-range interactions for four different types of oxygen pairs ($i=5$–8) are assumed to be characterized by only two parameters, A_5 and B_5. The latter is a reasonable approximation, because in most compounds it has been found[13,16–18] that the force constant associated with short-range, anion-anion interaction is much smaller than that associated with the usually dominant cation-anion interaction. The second term in Eq. (6), Φ^B, represents the three-body, bond-bending energy which reflects the covalency of atomic bonding. In the

valence-force-field approach, the harmonic part of this term can be written as[25]

$$\Phi^B=\tfrac{1}{2}\sum H_{ij}(R_{ij}\Delta\theta_{ij})^2 , \tag{8}$$

where $R_{ij}=(R_iR_j)^{1/2}$, θ_{ij} is the bond angle between R_i and R_j, and the summation is over all possible O-M-O and M-O-M interactions. We will further assume that the bond-bending force constant H_{ij} is a constant independent of equilibrium bond angle, i.e., a dimensionless parameter H will be defined as $H=(a^3/e^2)H_{ij}$.

We have obtained the equilibrium conditions by minimizing the total potential energy in Eq. (4) with respect to each of four structural parameters (i.e., a, c, u, and v) as follows:[26]

$$-z^2(M+rM_r)=(3v^2-3v+1)B_1+3v^2B_2+\tfrac{1}{2}B_4 +(\tfrac{45}{2}v^2-15v+\tfrac{9}{2})B_5 , \tag{9a}$$

$$z^2\frac{M_r}{r}=(3u^2-u+\tfrac{1}{12})B_1+3u^2B_2+2u^2B_3 +(6u^2-u+\tfrac{1}{24})B_4+\tfrac{1}{8}B_5 , \tag{9b}$$

$$z^2\frac{M_u}{r^2}=(3u-\tfrac{1}{2})B_1+3uB_2+2uB_3+(6u-\tfrac{1}{2})B_4 , \tag{9c}$$

$$z^2M_v=(3v-\tfrac{3}{2})B_1+3vB_2+(\tfrac{45}{2}v-\tfrac{15}{2})B_5 , \tag{9d}$$

where M_r, M_u, and M_v are the derivatives of M with respect to r, u, and v, respectively. The numerical values of M, M_r, M_u, and M_v listed in Table I were calculated by the usual Ewald method,[14] in which the convergence parameter was chosen for each compound by the criterion[27] that series in both the real and reciprocal lattices converge at the same rate as much as possible.

In addition to the effective-charge parameter z, the model contains eleven short-range parameters A_i, B_i, and H, where $i=1$–5. However, the total of 12 parameters can be reduced to eight independent, adjustable parameters by imposing the equilibrium conditions [Eq. (9)] as constraints.

C. Elastic constants and zone-center optical frequencies

The elastic constants $C_{\alpha\beta,\gamma\delta}$ in the rigid-ion approximation, as originally derived by Born and Huang[14] using the "method of long waves," can be expressed as

$$C_{\alpha\beta,\gamma\delta}=[\alpha\gamma,\beta\delta]+[\gamma\beta,\alpha\delta]-[\gamma\delta,\alpha\beta]+(\alpha\beta,\gamma\delta) , \tag{10}$$

where

$$[\alpha\gamma,\beta\delta]=\frac{1}{8\pi^2v_c}\sum_{k,k'}(m_km_{k'})^{1/2}\hat{D}^{(2)}_{\alpha\gamma,\beta\delta}(kk') , \tag{11}$$

$$(\alpha\beta,\gamma\delta)=-\frac{1}{v_c}\sum_{\lambda}\frac{F_{\alpha\beta}(\lambda)F_{\gamma\delta}(\lambda)}{\omega^2(\lambda)} , \tag{12}$$

and

$$F_{\alpha\beta}(\lambda)=\frac{1}{2\pi}\sum_{k',\mu}\left[\sum_k(m_k)^{1/2}\hat{D}^{(1)}_{\alpha\mu,\beta}(kk')\right]e_{\mu k'}(\lambda) . \tag{13}$$

The first three terms in square brackets and the last term in parentheses in Eq. (10) represent the external- and internal-strain contributions to the elastic constants, respectively. The notation $\hat{D}^{(n)}_{\alpha\beta,\gamma_1,\ldots,\gamma_n}$ denotes the nth-order derivative of the $\alpha\beta$th component of the dynamical matrix $\underline{\hat{D}}(\mathbf{q};kk')$ with respect to $q_{\gamma_1,\ldots,\gamma_n}$ at $\mathbf{q}=\mathbf{0}$ and the circumflex means that the macroscopic field has been removed. In the above equations, v_c is the unit-cell volume, m_k is the mass of the kth atom in the unit cell, and $\omega(\lambda)$ and $\underline{e}(\lambda)$ are frequency and eigenvector, respectively, of the λth optic mode at $\mathbf{q}=\mathbf{0}$. However, it will suffice to restrict our attention to the optic modes which are Raman-active because only these modes have nonvanishing contributions to the second-rank tensor $\overleftrightarrow{F}(\lambda)$, defined in Eq. (13), and hence to the internal-strain part of the elastic constants.[15]

The α-corundum structure has the symmetry of the D_{3d} point group, with its irreducible representations at zone center for the optic modes given as[28]

$$\Gamma=2A_{1g}+3A_{2g}+5E_g+2A_{1u}+2A_{2u}+4E_u , \tag{14}$$

where the A_{1g} and E_g representations contain Raman-active modes. The symmetry modes of these Raman-active species are shown in Fig. 2, following the results of a group-theoretical analysis carried out by Cowley[20] on the symmetry properties of the normal modes of vibration. The nonvanishing elements of $\overleftrightarrow{F}(\lambda)$, which has the same transformation properties as the Raman polarizability tensor $\overleftrightarrow{\alpha}(\lambda)$, are indicated below for each representation:[29]

$$A_{1g}:\begin{bmatrix} a & & \\ & a & \\ & & b \end{bmatrix},\quad E_g':\begin{bmatrix} c & & \\ & -c & d \\ & d & \end{bmatrix},\quad E_g'':\begin{bmatrix} & -c & -d \\ -c & & \\ -d & & \end{bmatrix}, \tag{15}$$

where the superscripts differentiate the degenerate modes of the two-dimensional representation E_g. Inspection of Eq. (12) and the structure of $\underline{F}$ matrices in Eq. (15) show that A_{1g} modes make internal-strain contributions to the elastic constants C_{11}, C_{12}, C_{13}, and C_{33}, but not to C_{44} or C_{14}, whereas E_g modes contribute to C_{11}, C_{12}, C_{44}, and C_{14}, but not to C_{13} or C_{33}.

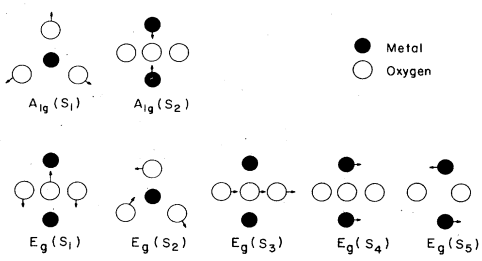

FIG. 2. The symmetry modes belonging to the Raman-active species A_{1g} and E_g according to Cowley (Ref. 20). Only the displacements of atoms in the upper half of a unit cell are shown, since those of atoms in the lower half follow inversion symmetry.

The frequencies and eigenvectors of Raman-active modes, which do not have a macroscopic electric field associated with their vibrational motions, can be determined without excessive labor by utilizing a set of symmetry modes for each irreducible representation. By expressing the eigenvector $\underline{e}$ as a linear combinations of all symmetry-adapted vectors $\underline{s}$ belonging to the same representation as

$$\underline{e}(\Gamma i)=\sum_{j=1}^{n_\Gamma} c(\Gamma i,\Gamma j)\underline{s}(\Gamma j)\ , \tag{16}$$

where n_Γ is the dimensionality of the representation Γ and $c(\Gamma i,\Gamma j)$ is the coefficient, the eigenvalue problem $\underline{D}^{(0)}\underline{e}=\omega^2\underline{e}$ is reduced to further diagonalizations of (2×2) and (5×5) submatrices, corresponding, respectively, to A_{1g} and E_g representations, of $\underline{D}^{\rm bl}=\underline{U}^\dagger\underline{\hat{D}}^{(0)}\underline{U}$, where $\underline{U}$ is a unitary matrix constructed by combining the $\underline{s}$'s columnwise and $\underline{D}^{\rm bl}$ is the block-diagonalized dynamical matrix.[25]

Using the explicit expressions for $\hat{D}^{(0)}_{\alpha\beta}$, $\hat{D}^{(1)}_{\alpha\beta,\gamma}$, and $\hat{D}^{(2)}_{\alpha\beta,\gamma\lambda}$,[14] the elastic constants in Eq. (10) can be rewritten in terms of model parameters as

$$C_{\mu\nu}=\frac{e^2}{2v_c a}\left[z^2Q_{\mu\nu}+\sum_{i=1}^{5}(\alpha^{(i)}_{\mu\nu}A_i+\beta^{(i)}_{\mu\nu}B_i)+\gamma_{\mu\nu}H\right]-\frac{1}{v_c}\sum_{\Gamma}\sum_{i=1}^{n_\Gamma}\frac{F_\mu(\Gamma i)F_\nu(\Gamma i)}{\omega^2(\Gamma i)}\ , \tag{17}$$

where $\mu,\nu=1$–6 (in Voigt's notation). The first term in large parentheses is due to the external strain and is a sum of Coulomb and short-range contributions. The numerical values of the Coulomb coefficients, $Q_{\mu\nu}$, are listed in Table II. The short-range coefficients $\alpha^{(i)}_{\mu\nu}$, $\beta^{(i)}_{\mu\nu}$, and $\gamma_{\mu\nu}$ are geometrical factors depending on the structural parameters and are also given in Table II. In order to conserve space, Tables II–VIII will contain values for $(V_{0.985}Cr_{0.015})_2O_3$ only. The double summation in the second term, the internal-strain contribution, is over all seven Raman-active modes ($n_\Gamma=2$ for $\Gamma=A_{1g}$ and $n_\Gamma=5$ for $\Gamma=E_g$), and $F_\mu(\Gamma i)$ can be written as

$$F_\mu(\Gamma i)=\sum_{j=1}^{n_\Gamma} c(\Gamma i,\Gamma j)G_\mu(\Gamma j)\ , \tag{18}$$

with

$$G_\mu(\Gamma j)=\frac{e^2}{a^2(m_0)^{1/2}}\left[z^2Q_\mu(\Gamma j)+\sum_{i=1}^{5}[\delta^{(i)}_\mu(\Gamma j)A_i+\epsilon^{(i)}_\mu(\Gamma j)B_i]+\lambda_\mu(\Gamma j)H\right]\ , \tag{19}$$

where m_0 is the mass of an oxygen atom and the coefficients $c(\Gamma i,\Gamma j)$ were defined in Eq. (16). The numerical values of the Coulomb coefficients Q_μ and short-range coefficients $\delta^{(i)}_\mu$, $\epsilon^{(i)}_\mu$, and λ_μ for the nonvanishing, independent elements of $\underline{G}(\Gamma j)$ [in accordance with the structure of $\underline{F}$ matrices in Eq. (15)] are listed in Table III for oxygen symmetry modes and in Table IV for metal symmetry modes. Finally, with the aforementioned (2×2) and (5×5) submatrices of $\underline{D}^{\rm bl}$ be-

TABLE II. Values of the Coulomb coefficients ($Q_{\mu\nu}$) and short-range coefficients ($\alpha^{(i)}_{\mu\nu}$, $\beta^{(i)}_{\mu\nu}$, and $\gamma_{\mu\nu}$) for $C_{\mu\nu}$ of $(V_{0.985}Cr_{0.015})_2O_3$. [Equation (17) shows how the coefficients occur in $C_{\mu\nu}$.]

$\mu\nu$	11	33	44	12	13	14
$Q_{\mu\nu}$	−7.515	99.173	−49.594	−114.234	−213.501	22.828
$\alpha^{(1)}_{\mu\nu}$	0.833	0.199	0.333	0.278	0.333	−0.058
$\alpha^{(2)}_{\mu\nu}$	0.474	0.804	0.504	0.158	0.504	0
$\alpha^{(3)}_{\mu\nu}$	0	1.208	0	0	0	0
$\alpha^{(4)}_{\mu\nu}$	1.468	0.002	0.042	0.489	0.042	0.144
$\alpha^{(5)}_{\mu\nu}$	5.049	5.116	1.328	1.683	1.328	−0.010
$\beta^{(1)}_{\mu\nu}$	0.611	0.666	0.532	−1.721	−1.777	0.058
$\beta^{(2)}_{\mu\nu}$	0.662	1.008	1.308	−1.294	−1.640	0
$\beta^{(3)}_{\mu\nu}$	0	0	1.208	0	0	0
$\beta^{(4)}_{\mu\nu}$	0.532	0.085	0.044	−2.489	−2.042	−0.144
$\beta^{(5)}_{\mu\nu}$	3.010	2.655	6.443	−9.742	−9.387	0.010
$\gamma_{\mu\nu}$	8.247	10.796	2.921	−2.849	−5.398	0.365

TABLE III. Values of the Coulomb coefficients (Q_μ) and short-range coefficients ($\delta_\mu^{(i)}$, $\varepsilon_\mu^{(i)}$, and λ_μ) for the nonvanishing, independent elements of $Q_\mu(\Gamma j)$ of $(V_{0.985}Cr_{0.015})_2O_3$ for oxygen symmetry modes. [Equation (19) shows how the coefficients occur in $G_\mu(\Gamma j)$.] For those symmetry modes in which only the oxygen atoms are in motion, $\delta_\mu^{(3)}=\delta_\mu^{(4)}=\varepsilon_\mu^{(3)}=\varepsilon_\mu^{(4)}=0$ for all μ.

$\Gamma(j)$:	$A_{1g}(S_1)$		$E_g(S_1)$		$E_g(S_2)$		$E_g(S_3)$	
μ:	1	3	1	4	1	4	1	4
Q_μ	39.653	−114.045	−90.715	−80.642	24.175	−128.290	−170.551	0
$\delta_\mu^{(1)}$	−0.513	−0.307	0.330	−0.217	−0.256	0.467	0.454	0
$\delta_\mu^{(2)}$	0.593	0.946	0	0.669	0.297	0	0.297	0
$\delta_\mu^{(5)}$	−0.514	−0.303	0.133	−0.214	−0.257	0.188	−0.574	0
$\varepsilon_\mu^{(1)}$	−0.154	0.307	−0.330	0.217	−0.410	−0.467	−0.454	0
$\varepsilon_\mu^{(2)}$	0.473	−0.946	0	−0.669	0.769	0	−0.297	0
$\varepsilon_\mu^{(5)}$	−0.152	0.303	−0.133	0.214	−0.409	−0.188	0.574	0
λ_μ	1.894	−3.789	−2.392	−0.936	2.046	−3.134	−5.387	0.249

ing defined as $\underline{d}(A_{1g})$ and $\underline{d}(E_g)$, respectively, the independent elements of these symmetric matrices, which upon diagonalization will give $\omega^2(\Gamma i)$ in Eq. (17) and $c(\Gamma i,\Gamma j)$ in Eq. (18), can also be expressed as a combination of Coulomb and short-range contributions as

$$d_n(\Gamma)=\frac{e^2}{m_0a^3}\left[z^2q_n(\Gamma)+\sum_{i=1}^{5}[\xi_n^{(i)}(\Gamma)A_i+\eta_n^{(i)}(\Gamma)B_i]+\zeta_n(\Gamma)H\right], \tag{20}$$

where $n=(\alpha\beta)$ with $\alpha\leq\beta$, i.e., $n=1$–3 for $\Gamma=A_{1g}$ and $n=1$–15 for $\Gamma=E_g$. The numerical values of q_n, $\xi_n^{(i)}$, $\eta_n^{(i)}$, and ζ_n are listed in Table V for $\underline{d}(A_{1g})$ and in Table VI for $\underline{d}(E_g)$. The various Coulomb coefficients presented in Tables II–VI were also calculated using Ewald's method mentioned earlier.

III. DATA AND CALCULATION

The experimental values of the room-temperature elastic constants were taken from Nichols and Sladek[11] for V_2O_3, from Yang *et al.*[12] for $(V_{0.985}Cr_{0.015})_2O_3$, and from Gieske and Barsch[30] for Al_2O_3, while those of Raman frequencies are from Fan *et al.*[8,9] for V_2O_3 and $(V_{0.985}Cr_{0.015})_2O_3$ (although only four of the five E_g modes were reported for these compounds) and from Porto and Krishnan[31] for Al_2O_3.

The eight independent parameters of the model were determined from a nonlinear least-squares fit to all available elastic and Raman data. This calculation was performed on a computer using the International Mathematical and Statistical Library subroutine ZXMWD, which minimized the sum of squares of the relative deviation of the

TABLE IV. The same as described in the caption of Table III, for metal symmetry modes. For those modes in which only the metal atoms are in motion, $\delta_\mu^{(5)}=\varepsilon_\mu^{(5)}=0$ for all μ.

$\Gamma(j)$:	$A_{1g}(S_2)$		$E_g(S_4)$		$E_g(S_5)$	
μ:	1	3	1	4	1	4
Q_μ	−6.467	−2.263	−28.121	0	27.521	0
$\delta_\mu^{(1)}$	0.347	0.208	0.311	0	0.061	−0.347
$\delta_\mu^{(2)}$	−0.363	−0.579	−0.204	0	0	0.363
$\delta_\mu^{(3)}$	0	−0.871	0	0	0	0
$\delta_\mu^{(4)}$	−0.198	−0.009	0	0	0.672	0.198
$\varepsilon_\mu^{(1)}$	−0.347	0.695	−0.311	0	−0.061	−0.555
$\varepsilon_\mu^{(2)}$	0.363	−0.727	0.204	0	0	0.943
$\varepsilon_\mu^{(3)}$	0	0	0	0	0	0.871
$\varepsilon_\mu^{(4)}$	0.198	−0.395	0	0	−0.672	0.206
λ_μ	0.538	−1.076	−1.361	−0.812	0.017	1.123

TABLE V. Values of the Coulomb coefficients (q_n) and short-range coefficients ($\xi_n^{(i)}$, $\eta_n^{(i)}$, and ζ_n) for the independent elements of the symmetric (2×2) matrix $\underline{d}(A_{1g})$ of $(V_{0.985}Cr_{0.015})_2O_3$. [Equation (20) shows how the coefficients occur in $d_n(\Gamma)$.]

n:	1	2	3
$(\alpha\beta)$:	(11)	(21)	(22)
q_n	−19.204	238.659	0.028
$\xi_n^{(1)}$	0.473	−0.320	0.217
$\xi_n^{(2)}$	1.113	−0.682	0.418
$\xi_n^{(3)}$	0	0	0.628
$\xi_n^{(4)}$	0	0	0.040
$\xi_n^{(5)}$	5.235	0	0
$\eta_n^{(1)}$	1.527	0.320	0.725
$\eta_n^{(2)}$	0.887	0.682	0.524
$\eta_n^{(3)}$	0	0	0
$\eta_n^{(4)}$	0	0	1.844
$\eta_n^{(5)}$	9.765	0	0
ζ_n	11.668	5.994	6.235

calculated and observed quantities with respect to a set of unknown parameters. In the fitting process, we noted the following.

(1) The dimensionless quantities $(2v_c a/e^2)C_{\mu\nu}$ and $(m_0 a^3/e^2)\omega^2(\Gamma i)$ were used to treat the elastic constants and Raman frequencies on an equal footing.

(2) A considerably smaller weight was given to the C_{14} elastic constant since the absolute value of C_{14} is about 1–2 orders of magnitude smaller than those of other $C_{\mu\nu}$'s.

(3) The C_{44} elastic constant was not used in the case of $(V_{1-x}Cr_x)_2O_3$ since its anomalous temperature dependence indicated[32] that even at room temperature it is significantly affected by the low-temperature structural phase transition.

(4) The E_g mode not observed experimentally for V_2O_3 and $(V_{1-x}Cr_x)_2O_3$ was assumed to have the fourth-highest frequency among E_g modes, in accordance with the Raman spectra of other corundum-structured sesquioxides.[31,33–35]

IV. RESULTS AND DISCUSSIONS

The numerical values of the elastic constants and Raman frequencies, calculated from the best-fit parameters

TABLE VI. The same as described in the caption of Table V for the independent elements of the symmetric (5×5) matrix $\underline{d}(E_g)$. It is noted that $\xi_n^{(3)}=\eta_n^{(3)}=\xi_n^{(4)}=\eta_n^{(4)}=0$ for all n from 1 to 7 and $\xi_n^{(3)}=\xi_n^{(5)}=\eta_n^{(5)}=0$ for all n from 8 to 15.

n:	1	2	3	4	5	6	7
$(\alpha\beta)$:	(11)	(21)	(22)	(31)	(32)	(33)	(41)
q_n	−31.199	41.308	15.580	−106.344	−58.143	−109.282	−95.933
$\xi_n^{(1)}$	0.461	−0.496	0.769	0.496	−0.296	0.769	0.340
$\xi_n^{(2)}$	0.887	0	0.556	0	0.556	0.556	0
$\xi_n^{(5)}$	4.047	−1.778	5.476	0.085	−0.172	2.050	0
$\eta_n^{(1)}$	1.539	0.496	1.231	−0.496	0.296	1.231	−0.340
$\eta_n^{(2)}$	1.113	0	1.444	0	−0.556	1.444	0
$\eta_n^{(5)}$	10.953	1.778	9.524	−0.085	0.172	9.950	0
ζ_n	11.892	2.201	13.928	1.934	−1.619	9.053	−1.854
n:	8	9	10	11	12	13,14	15
$(\alpha\beta)$:	(42)	(43)	(44)	(51)	(52)	(53,54)	(55)
q_n	166.912	−46.883	23.101	−168.757	141.843	0	−0.031
$\xi_n^{(1)}$	−0.203	0.528	0.362	0.227	−0.487	0	0.362
$\xi_n^{(2)}$	−0.382	−0.382	0.262	0.482	0	0	0.262
$\xi_n^{(4)}$	0	0	0.922	0	0	0	.922
$\eta_n^{(1)}$	0.203	0.844	0.580	−0.227	0.487	0	0.580
$\eta_n^{(2)}$	0.382	−0.991	0.680	−0.482	0	0	0.680
$\eta_n^{(3)}$	0	0	0	0	0	0	.628
$\eta_n^{(4)}$	0	0	0.962	0	0	0	0.962
ζ_n	2.489	0.341	5.388	−4.004	2.570	a	5.722

[a] $\zeta_{13}=-0.338$ and $\zeta_{14}=1.629$.

TABLE VII. Experimental and calculated $C_{\mu\nu}$ (in units of 10^{11} dyn/cm^2) and $\omega_{\Gamma(i)}$ (in units of cm^{-1}) for V_2O_3, $(V_{0.985}Cr_{0.015})_2O_3$, and Al_2O_3.

	V_2O_3		$(V_{0.985}Cr_{0.015})_2O_3$		Al_2O_3	
	Expt.	Calc.	Expt.	Calc.	Expt.	Calc.
C_{11}	27.1	26.1	28.7	28.7	49.8	52.4
C_{33}	34.0	31.7	33.9	30.9	50.2	47.9
C_{44}	8.5	10.2	5.7	10.9	14.7	14.7
C_{12}	8.2	8.7	10.5	10.6	16.3	16.0
C_{13}	14.7	13.6	15.4	14.5	11.7	11.6
C_{14}	−1.9	−0.2	−0.3	−0.1	−2.3	−2.2
$\omega_{A_{1g}(1)}$	234	243	249	257	418	420
$\omega_{A_{1g}(2)}$	501	562	516	572	645	674
$\omega_{E_g(1)}$	210	217	210	222	378	382
$\omega_{E_g(2)}$	296	247	310	253	432	413
$\omega_{E_g(3)}$	327	317	337	337	451	460
$\omega_{E_g(4)}$		378		408	578	534
$\omega_{E_g(5)}$	595	652	600	655	751	772

of the model, are compared with experimental data in Table VII for V_2O_3, $(V_{0.985}Cr_{0.015})_2O_3$, and Al_2O_3. The overall agreement between the calculated and observed quantities is fairly good for all three compounds, the results differing by less than 10% for both V_2O_3 and $(V_{0.985}Cr_{0.015})_2O_3$ and by less than 5% for Al_2O_3 in most cases. There are, however, a few exceptions in $(V_{1-x}Cr_x)_2O_3$, including $\omega_{E_g}(2)$, for which the calculated values are about 15–20% smaller than the experimental values, and, of course, C_{44}, which was not considered in the fitting process, as already mentioned in the preceding section. The calculated values of C_{44} in $(V_{1-x}Cr_x)_2O_3$, which are considerably larger than what were observed, are, in fact, what one would expect if there were no low-temperature structural phase transitions in these compounds. It should be noted that the only previous attempt to fit both the elastic constants and optical frequencies in a corundum-structured sesquioxide was made by Iishi[17] on Al_2O_3 using a simple short-range force model. However, the values he calculated for the elastic constants were not close to the experimental data. The reasonable success of our model in reproducing not only the optical frequencies but also the elastic constants, therefore, would imply that the contribution from Coulomb interactions is significant for the elastic constants as well as for the optical frequencies. It is also noteworthy that in view of the relatively worse overall agreement between the calculated and observed quantities in $(V_{1-x}Cr_x)_2O_3$, which contains d electrons, than in Al_2O_3, an attempt was made to include the effect of the presence of d electrons in the model for $(V_{1-x}Cr_x)_2O_3$. The simplest method was to replace the $1/r$ of the Coulomb interaction by $\exp(-\alpha r)/r$,[36] where α is the Thomas-Fermi reciprocal screening length due to the presence of d electrons. However, the resulting modification of various Coulomb coefficients in the model for several trial values of αr did not improve the fit significantly in $(V_{1-x}Cr_x)_2O_3$. This is not too surprising considering the highly directional character of d-electron orbitals, and it seems that, to have any reasonable success at all, one might have to consider an anisotropic screening which would render the problem much more complicated as well as introducing additional parameters into the model.

The eigenvectors for each Raman-active mode obtained from the least-squares fit are listed in Table VIII for $(V_{0.985}Cr_{0.015})_2O_3$. These eigenvectors, together with the symmetry modes in Fig. 2, give information about the vibrational mode of each optical frequency. The A_{1g}

TABLE VIII. Values of the coefficient $c(\Gamma i,\Gamma j)$ [see Eq. (16)] for the eigenvectors $\underline{e}(\Gamma i)$ determined from the least-squares fit of the model for $(V_{0.985}Cr_{0.015})_2O_3$.

	S_1	S_2	S_3	S_4	S_5
$A_{1g}(1)$	0.086	0.996			
$A_{1g}(2)$	−0.996	0.086			
$E_g(1)$	−0.113	−0.024	−0.047	−0.055	0.991
$E_g(2)$	−0.116	−0.111	−0.049	0.983	−0.068
$E_g(3)$	0.576	0.303	−0.749	0.072	0.105
$E_g(4)$	−0.533	−0.526	−0.643	−0.157	−0.034
$E_g(5)$	−0.598	0.786	−0.146	0.008	−0.043

mode with lower frequency (A_{1g}^{L}), for example, can be described as a breathing mode in which the metal atoms move toward each other along the c axis while the oxygen triangle moves outward in the basal plane. In the higher-frequency A_{1g} mode (A_{1g}^{H}), the inward motion of oxygen triangle is in phase with that of the metal pair. These descriptions of the A_{1g} modes, which would imply that the A_{1g}^{L} mode produces a larger modulation of the trigonal component of the crystal field than does the A_{1g}^{H} mode, are consistent with the interpretation of the stronger relative intensity[33] (or the larger magnitude of the resonance enhancement in Raman scattering[37]) of the A_{1g}^{L} mode compared to the A_{1g}^{H} mode in Ti_2O_3.

The numerical values of the effective charge of the metal ion, Z_M ($=3z\,|\,e\,|$), and various short-range force constants derived from the best-fit model parameters for V_2O_3, $(V_{0.985}Cr_{0.015})_2O_3$, and Al_2O_3, and Al_2O_3, are listed in Table IX. First of all, in the case of Al_2O_3, one could compare some of the results in Table IX with those from other rigid-ion (RI) or polarizable-ion (PI) models, bearing in mind the different approaches used in these models. The effective charge of the aluminum ion, Z_{Al}, has quite a spread in its values: 1.67 in this model compared to 1.43 (RI, Iishi[17]), 2.05 (RI, Kappus[16]), and 1.80 (PI, Lauwers *et al.*[18]). It is surprising but satisfying that the value of 1.67 for Z_{Al} compares most favorably with that of 1.72 evaluated[38] from the experimental TO-LO splitting in the infrared frequencies, despite the fact that infrared-active modes were not considered in the present model. The short-range force constants of Al_2O_3 are generally comparable in magnitude to those from other models. The strong force constants associated with Al-O bond stretching are 81.0 and 43.9 in units of e^2/a^3, or 1.74×10^5 and 0.94×10^5 dyn/cm, which are comparable to the average value of 1.27×10^5 dyn/cm (RI, Iishi), but are substantially smaller than that of 1.96×10^5 dyn/cm (RI, Kappus) or 1.85×10^5 dyn/cm (PI, Lauwers *et al.*). The average force constant associated with the O-O repulsion, $19.2(e^2/a^3)=0.41\times10^5$ dyn/cm, is larger than the values of 0.16×10^5, 0.09×10^5, and 0.07×10^5 dyn/cm quoted by Iishi, Kappus, and Lauwers *et al.*, respectively, while the force constants associated with Al-Al interactions are by no means negligible in this model. This is unlike the results of other investigators, who simply neglected them (Iishi and Kappus) or found no evidence for the metal-metal interaction (Lauwers *et al*).

In the case of $(V_{1-x}Cr_x)_2O_3$, as can be seen in Table IX, the much larger values of Z_M than in Al_2O_3, together with the negligible values of H, suggest that these compounds might be more ionic than Al_2O_3. While no other estimates of the effective charge or ionicity of $(V_{1-x}Cr_x)_2O_3$ to support the current results are available in the literature, we note that Levine[39] has extended the dielectric theory of ionicity, developed by Phillips and Van Vechten[40] for the simple A^NB^{8-N} compounds, to more complex crystals, including transition-metal compounds containing d electrons. We have therefore utilized Levine's method to estimate the ionicity of V_2O_3 from

TABLE IX. Effective charge of metal ion and various short-range force constants derived from the best-fitting model parameters for V_2O_3, $(V_{0.985}Cr_{0.015})_2O_3$, and Al_2O_3. The values of Z_M are given in units of $|\,e\,|$ and those of A_i, B_i, and H are in units of e^2/a^3. Also listed is the ionicity, f_i, for V_2O_3 and Al_2O_3.

		V_2O_3	$(V_{0.985}Cr_{0.015})_2O_3$	Al_2O_3
Z_M		2.38	2.08	1.67
f_i		0.86[a]		0.80[b]
$M(1)$-O(4)	A_1	139.7	124.4	81.0
	B_1	−30.1	−25.2	−26.6
$M(1)$-O(1)	A_2	112.6	96.7	43.9
	B_2	−24.1	−18.6	−15.8
$M(1)$-$M(2)$	A_3	−36.3	−15.0	25.1
	B_3	9.4	5.0	0.0
$M(1)$-$M(3)$	A_4	−35.4	−25.2	5.8
	B_4	5.0	3.0	1.0
O(1)-O(k)[c]	A_5	7.2	9.6	19.2
	B_5	1.2	1.3	3.4
O-M-O + M-O-M	H	0.0	0.0	2.9

[a]Estimated following Levine's method (Ref. 38) with $\epsilon_\infty=3.75$.
[b]Reference 38.
[c]$k=2$, 4, 5, and 6.

structural data and the electronic dielectric constant $\epsilon_\infty = 3.75$ determined from the reflectivity-spectra measurements.[41] This value of ionicity, f_i, for V_2O_3, is also listed in Table IX, together with the ionicity of Al_2O_3 given by Levine.[39] Although there exists no rigorous relation between ionicity and effective charge, it is clear that $f_i(V_2O_3) > f_i(Al_2O_3)$ is consistent with the result of current model: $Z_V > Z_{Al}$. It can also be seen from Table IX that the short-range force constants of $(V_{1-x}Cr_x)_2O_3$ crystals are quite different from those of Al_2O_3. The M-O stretching force constants (A_1 and A_2) of $(V_{1-x}Cr_x)_2O_3$, for example, are considerably larger than those of Al_2O_3 despite the fact that the latter has the shortest M-O distances among all the isostructural sesquioxides. Certainly, one cannot expect close similarity between the force constants of the compounds considered here because of large differences in the electronic configurations of the cations. Although it is tempting to attribute the strong M-O force constants of $(V_{1-x}Cr_x)_2O_3$ to the presence of d electrons, they might be a consequence of relatively higher ionicities of M-O bonding in these compounds. On the other hand, the alloying of a small amount of Cr_2O_3 into V_2O_3 is seen to have the effect of decreasing the effective ionic charge as well as of decreasing the strength of most of the short-range forces. The latter is in accordance with the interatomic distances of $(V_{0.985}Cr_{0.015})_2O_3$ being generally larger than those of pure V_2O_3.[22] Concerning the M-M interactions in V_2O_3 and $(V_{0.985}Cr_{0.015})_2O_3$, it is of interest to note that, as can be seen in Table IX, the force constants A_3 and A_4 are negative while B_3 and B_4 are positive. In view of the definitions of the A_i's and B_i's in terms of the second and first derivatives, respectively, of the short-range potential with respect to the interatomic distance R_i [see Eq. (7)], it is clear that the short-range potential for each of these M-M pairs in the $(V_{1-x}Cr_x)_2O_3$ crystals cannot be represented by a simple inverse-power (or Born-Mayer) repulsive potential alone, but has to include an attractive term similar to the van der Waals—type interaction[42] commonly used for molecular crystals. However, this sign reversal for both A_i and B_i is not too unusual for a pair of like atoms which are relatively far apart (i.e., beyond the nearest neighbors), since similar results have been reported for the F-F interactions in BaF_2 (Ref. 43) and PbF_2 (Ref. 44), for the Sn-Sn interaction in SnTe (Ref. 45), and for the Sb-Sb interaction in NdSb (Ref. 46). On the other hand, the positive values of B_i for the M-M interactions in Al_2O_3 and for the O-O interactions in all three compounds do not present a serious problem since they are negligibly small and, in the case of O-O interactions, this may have been caused by using only one set of parameters for all four pairs of oxygens although the O-O separations of these pairs are slightly different from each other. Also interesting is the fact that the effective charge and most of the short-range force constants for semiconducting $(V_{0.985}Cr_{0.015})_2O_3$ have values in between those of metallic V_2O_3 and insulating Al_2O_3, although it is difficult to correlate microscopic force-field parameters with the degree of itinerancy of charge carriers, if any, in these compounds.

V. CONCLUSION

A lattice-dynamical model based on a rigid-ion approximation with an effective ionic charge and short-range interactions between near-neighbor atoms has been used to reproduce quite successfully not only the experimental Raman frequencies but also the elastic constants of V_2O_3 and $(V_{0.985}Cr_{0.015})_2O_3$, as well as of Al_2O_3. The effective ionic charge of each of our $(V_{1-x}Cr_x)_2O_3$ crystals is found to be substantially larger than that of Al_2O_3. This result is consistent with the ionicity of V_2O_3, estimated using an extended dielectric theory of Levine, being larger than that of Al_2O_3. The short-range force constants of $(V_{1-x}Cr_x)_2O_3$ are found to be quite different from those of Al_2O_3, probably due to the large differences in the electronic configurations of the cations. The alloying of a small amount of Cr_2O_3 into V_2O_3, which is known to produce a metal-to-semiconductor transition but not to affect the lattice properties significantly, is found to result in a systematic variation in the effective charge and various short-range force constants. The latter is attributed to the changes in interatomic distances.

ACKNOWLEDGMENT

This work was supported in part by the National Science Foundation via Materials Research Program Grant No. DMR-80-20249.

[1]For a review of various properties of $(V_{1-x}Cr_x)_2O_3$, see, for example, J. M. Honig and L. L. Van Zandt, in *Annual Review of Materials Science*, edited by R. Huggins, R. H. Bube, and R. W. Roberts (Annual Reviews, Inc., Palo Alto, CA, 1975), Vol. 5, p. 255; Ref. 2, and the references cited therein.

[2]H. Kuwamoto, J. M. Honig, and J. Appel, Phys. Rev. B **22**, 2626 (1980).

[3]D. B. McWhan and J. P. Remeika, Phys. Rev. B **2**, 3734 (1970).

[4]M. S. Kozyreva, V. N. Novikov, and B. A. Tallerchik, Fiz. Tverd. Tela (Leningrad) **14**, 749 (1972) [Sov. Phys.—Solid State **14**, 639 (1972)].

[5]A. S. Barker, Jr. and J. P. Remeika, Solid State Commun. **8**, 1521 (1970).

[6]W. B. Yelon and J. E. Keem, Solid State Commun. **29**, 775 (1979).

[7]M. Yethiraj, S. A. Werner, W. B. Yelon, and J. M. Honig, in *Neutron Scattering—1981 (Argonne National Laboratory)*, edited by John Farber, Jr. (AIP, New York, 1982), p. 343.

[8]N. Kuroda and H. Y. Fan, Phys. Rev. B **16**, 5003 (1977).

[9]C. Tatsuyama and H. Y. Fan, Phys. Rev. B **21**, 2977 (1980).

[10]I. L. Drichko and S. I. Kogan, Fiz. Tverd. Tela (Leningrad) **16**, 1015 (1974) [Sov. Phys.—Solid State **16**, 656 (1974)].

[11]D. N. Nichols and R. J. Sladek, Phys. Rev. B **24**, 3155 (1981).

[12]H. Yang, R. J. Sladek, and H. R. Harrison, Phys. Rev. B **31**, 5417 (1985).

[13]M. E. Striefler and G. R. Barsch, Phys. Status Solidi B **59**, 205 (1973).
[14]M. Born and K. Huang, *Dynamical Theory of Crystal Lattices* (Oxford University Press, London, 1954), Chap. V.
[15]P. B. Miller and J. D. Axe, Phys. Rev. **163**, 924 (1967).
[16]W. Kappus, Z. Phys. B **21**, 325 (1975).
[17]K. Iishi, Phys. Chem. Miner. **3**, 1 (1978).
[18]H. A. Lauwers, L. Van Haverbeke, and M. A. Herman, J. Phys. Chem. Solids **44**, 489 (1983).
[19]S. H. Shin, Ph.D. thesis, Purdue University, 1972 (unpublished).
[20]E. R. Cowley, Can. J. Phys. **47**, 1381 (1969).
[21]W. R. Robinson, Acta Crystallogr. Sect. B **31**, 1153 (1975).
[22]S. Chen, J. E. Hahn, C. E. Rice, and W. R. Robinson, J. Solid State Chem. **44**, 192 (1982).
[23]R. E. Newnham and Y. M. de Haan, Z. Kristallogr. **117**, 235 (1962).
[24]R. S. Katiyar, J. Phys. C **3**, 1693 (1970).
[25]G. Venkataraman, L. A. Feldkamp, and V. C. Sahni, *Dynamics of Perfect Crystals* (MIT Press, Cambridge, MA, 1975), p. 20.
[26]The first derivatives of the bond-bending term in Eq. (8) with respect to the structural parameters are assumed to be zero in the harmonic approximation.
[27]W. Van Gool and A. G. Piken, J. Mater. Sci. **4**, 95 (1969).
[28]S. Bhagavantam and T. Venkatarayudu, Proc. Indian Acad. Sci. A **9**, 224 (1939).
[29]R. Loudon, Adv. Phys. **13**, 423 (1964).
[30]J. H. Gieske and G. R. Barsch, Phys. Status Solidi **29**, 121 (1968).
[31]S. P. S. Porto and R. S. Krishnan, J. Chem. Phys. **47**, 1009 (1967).
[32]H. Yang, R. J. Sladek, and H. R. Harrison, Solid State Commun. **47**, 955 (1983).
[33]A. Mooradian and P. M. Raccah, Phys. Rev. B **3**, 4253 (1971).
[34]S. H. Shin, R. L. Aggarwal, B. Lax, and J. M. Honig, Phys. Rev. B **9**, 583 (1974).
[35]T. R. Hart, R. L. Aggarwal, and B. Lax, in *Light Scattering in Solids,* edited by M. Balkanski (Flammarion, Paris, 1971), p. 174.
[36]N. F. Mott and H. Jones, *The Theory of the Properties of Metals and Alloys* (Oxford University Press, London, 1936), p. 41.
[37]S. H. Shin, F. H. Pollak, T. Halpern, and P. M. Raccah, Solid State Commun. **16**, 687 (1975).
[38]F. Gervais, Solid State Commun. **18**, 191 (1976).
[39]B. F. Levine, Phys. Rev. B **7**, 2591 (1973).
[40]See, for example, J. C. Phillips, Phys. Rev. Lett. **20**, 550 (1968); Rev. Mod. Phys. **42**, 317 (1970); J. A. Van Vechten, Phys. Rev. **182**, 891 (1969).
[41]V. P. Zhuze, D. P. Lukirskii, and G. P. Startsev, Fiz. Tverd. Tela (Leningrad) **13**, 317 (1971) [Sov. Phys.—Solid State **13**, 260 (1971)].
[42]*Dynamical Theory of Crystal Lattices,* Ref. 14, Chap. I.
[43]J. D. Axe, Phys. Rev. **139**, A1215 (1965).
[44]M. H. Dickens and M. T. Hutchings, in *Lattice Dynamics,* edited by M. Balkanski (Flammarion, Paris, 1978), p. 540.
[45]E. R. Cowley, J. K. Darby, and G. S. Pawley, J. Phys. C **2**, 1916 (1969).
[46]N. Wakabayashi and A. Furrer, Phys. Rev. B **13**, 4343 (1976).